Article

Hopping Transport in Conductive Heterocyclic Oligomers: Reorganization Energies and Substituent Effects

Geoffrey R. Hutchison, Mark A. Ratner, and Tobin J. Marks

J. Am. Chem. Soc., **2005**, 127 (7), 2339-2350• DOI: 10.1021/ja0461421 • Publication Date (Web): 01 February 2005

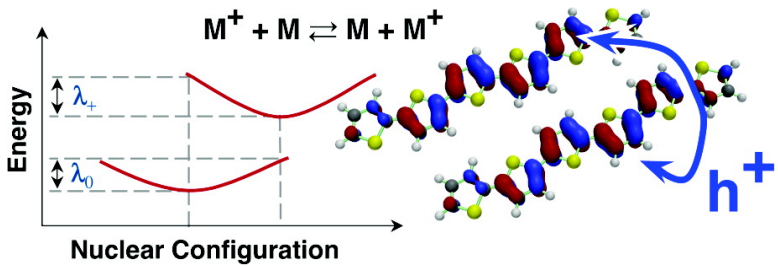

More About This Article

Additional resources and features associated with this article are available within the HTML version:

- Supporting Information
- Links to the 32 articles that cite this article, as of the time of this article download
- Access to high resolution figures
- Links to articles and content related to this article
- Copyright permission to reproduce figures and/or text from this article

View the Full Text HTML

J|A|C|S
ARTICLES
Published on Web 02/01/2005

Hopping Transport in Conductive Heterocyclic Oligomers: Reorganization Energies and Substituent Effects

Geoffrey R. Hutchison,† Mark A. Ratner,* and Tobin J. Marks*

Contribution from the Department of Chemistry and the Materials Research Center, Northwestern University, Evanston, Illinois 60208-3113

Received June 29, 2004; E-mail: ratner@chem.northwestern.edu; t-marks@northwestern.edu

Abstract: Molecular scale charge motion in disordered organic materials at ambient temperature occurs via a hopping-type mechanism with rates dictated both by the charge transfer integral and by the reorganization energy due to geometric relaxation. This contribution presents a systematic theoretical analysis of cation internal reorganization energies for a broad family of organic oligoheterocycles—variation of reorganization energy with oligomer chain length, heteroatom identity, and a range of heterocycle substituents provides key information on important structural properties governing internal reorganization energies. At room temperature, the range in reorganization energies induced by substituent variations corresponds to a $>10^2$-fold variation in intrinsic hole transfer rate, suggesting that changes in reorganization energy dominate variations in charge-transfer rates for many semiconducting/conducting oligomers.

I. Introduction

Conjugated organic π-electron materials are of immense interest, both for intrinsic scientific challenges they pose and for potential applications, particularly for the wide variety of semiconducting and conducting properties useful in light-emitting diodes,[1] photovoltaics,[2] field-effect transistors,[3] and other elements of "plastic electronics." The mechanisms of conductivity in organic materials over nanoscopic and mesoscopic ranges are currently the focus of intense research and likely differ substantially for different systems.[4,5] On the molecular scale, as in charge-transfer in many other molecular systems, most conjugated oligomers and polymers are assumed to transport charge at room temperature via a thermally activated hopping-type mechanism.[5] Extensive experimental evidence, particularly the observed thermal signatures, and optical spectra, are consistent with this assumption.[5−9]

The vast majority of organic conductive materials are *p*-type, so the hole-transfer process between adjacent spatially separated molecules can be summarized as follows:

$$M + M^+ \rightarrow M^+ + M \qquad (1)$$

where M represents the neutral species undergoing charge transfer, and the M^+ species contains the hole. Two key parameters are the reorganization energy (λ) due to geometric relaxation accompanying charge transfer and the electronic coupling matrix element (V) between the two species, dictated largely by orbital overlap. The latter is akin to the bandwidth in conventional solid-state descriptions, and in a tight-binding model, the bandwidth is twice the orbital energy splitting observed in a dimeric pair, or four times the charge-resonance integral β. Brédas and co-workers have studied orbital energy splittings and bandwidths using semiempirical methods in a

† New address: Department of Chemistry and Chemical Biology, Cornell University, Baker Laboratory, Ithaca, New York 14853-1301.

(1) (a) Ho, P. K. H.; Kim, J.-S.; Burroughes, J. H.; Becker, H.; Li, S. F. Y.; Brown, T. M.; Cacialli, F.; Friend, R. H. *Nature* **2000**, *404*, 481. (b) Pinner, D. J.; Friend, R. H.; Tessler, N. *Appl. Phys. Lett.* **2000**, *76*, 1137. (c) Inganäs, O.; Berggren, M.; Andersson, M. R.; Gustafsson, G.; Hjertberg, T.; Wennerström, O.; Dyreklev, P.; Granström, M. *Synth. Met.* **1995**, *71*, 2121.
(2) (a) Ding, L.; Jonforsen, M.; Roman, L. S.; Andersson, M. R.; Inganäs, O. *Synth. Met.* **2000**, *110*, 113. (b) Granström, M.; Petrisch, K.; Arias, A. C.; Lux, A.; Andersson, M. R.; Friend, R. H. *Nature* **1998**, *395*, 257.
(3) (a) Würthner, F. *Angew. Chem., Int. Ed. Engl.* **2001**, *40*, 1037. (b) Garnier, F. *Chem. Phys.* **1998**, *227*, 253. (c) Katz, H. E. *J. Mater. Chem.* **1997**, *7*, 369.
(4) (a) Prigodin, V. N.; Epstein, A. J. *Synth. Met.* **2001**, *125*, 43. (b) Joo, J.; Lee, J. K.; Baeck, J. S.; Kim, K. H.; Oh, E. J.; Epstein, J. *Synth. Met.* **2001**, *117*, 45. (c) Hilt, O.; Reedijk, J. A.; Martens, H. C. F.; Brom, H. B.; Michels, M. A. J. *Phys. Status Solidi B* **2000**, *218*, 279. (d) Reedijk, J. A.; Martens, H. C. F.; Brom, H. B.; Michels, M. A. J. *Phys. Rev. Lett.* **1999**, *83*, 3904. (e) Kohlman, R. S.; Epstein, A. J. In *Handbook of Conducting Polymers*; 2nd ed.; Skotheim, T. A., Elsenbaumer, R. L., Reynolds, J. R., Eds.; Marcel Dekker: New York, 1998; pp 85. (f) Menon, R.; Yoon, C. O.; Moses, D.; Heeger, A. J. In *Handbook of Conducting Polymers*, 2nd ed.; Skotheim, T. A., Elsenbaumer, R. L., Reynolds, J. R., Eds.; Marcel Dekker: New York, 1998, pp 27. (g) Epstein, A. J. *Mater. Res. Bull.* **1997**, *22*, 16. (h) Pope, M.; Swenberg, C. E. *Electronic Processes in Organic Crystals and Polymers*, 2nd ed.; Oxford University Press: New York, 1999. (i) Pope, M.; Swenberg, C. E. *Electronic Processes in Organic Crystals*; Oxford University Press: New York, 1982.
(5) (a) Epstein, A. J.; Lee, W. P.; Prigodin, V. N. *Synth. Met.* **2001**, *117*, 9. (b) Reedijk, J. A.; Martens, H. C. F.; van Bohemen, S. M. C.; Hilt, O.; Brom, H. B.; Michels, M. A. J. *Synth. Met.* **1999**, *101*, 475. (c) Mott, N. F.; Davis, E. A. *Electronic Processes in Non-Crystalline Materials*; 2d ed.; Oxford University Press: Oxford, 1979.
(6) (a) Romijin, I. G.; Pasveer, W. F.; Martens, H. C. F.; Brom, H. B.; Michels, M. A. J. *Synth. Met.* **2001**, *119*, 439. (b) Brom, H. B.; Reedijk, J. A.; Martens, H. C. F.; Adriaanse, L. J.; De Jongh, L. J.; Michels, M. A. J. *Phys. Status Solidi B* **1998**, *205*, 103. (c) Wegner, G.; Ruehe, J. *Faraday Discuss.* **1989**, *88*, 333.
(7) Granstrom, E. L.; Frisbie, C. D. *J. Phys. Chem. B* **1999**, *103*, 8842.
(8) (a) de Boer, R. W. I.; Jochemsen, M.; Klapwijk, T. M.; Morpurgo, A. F.; Niemax, J.; Tripathi, A. K.; Pflaum, J. *J. Appl. Phys.* **2004**, *95*, 1196. (b) Schein, L. B.; Duke, C. B.; Mcghie, A. R. *Phys. Rev. Lett.* **1978**, *40*, 197. (c) Kondrasiuk, J.; Szymanski, A. *Mol. Cryst. Liq. Cryst.* **1972**, *18*, 379. (d) Bogus, C. Z. *Phys.* **1965**, *184*, 219. (e) Bryant, F. J.; Bree, A.; Fielding, P. E.; Schneider, W. G. *Faraday Discuss.* **1959**, *28*, 48.
(9) Nam, M. S.; Ardavan, A.; Cava, R. J.; Chaikin, P. M. *Appl. Phys. Lett.* **2003**, *83*, 4782.

variety of conjugated organic materials and the effects of structural perturbations on orbital splittings and hence, the charge-transfer rates.[10] We have also recently investigated orbital energy splittings in oligoheterocycles and the consequences for charge-transfer rates using first-principles calculations.[11] However, while the importance of reorganization energy in charge transfer processes has been heavily studied in solution-phase reactions in the context of Marcus theory,[12−14] and more recently for molecular wires,[15,16] few detailed studies exist for solid-phase organic conductors.[17]

If the temperature is sufficiently high to treat vibrational modes classically, then the standard Marcus/Hush model yields the following expression for the hole (or electron) charge-transfer rate, assuming that hole traps are degenerate:[14,15,18]

$$k_{\text{hole}} = \left(\frac{\pi}{\lambda k_b T}\right)^{1/2} \frac{V^2}{\hbar} \exp\left(-\frac{\lambda}{4k_b T}\right) \qquad (2)$$

where T is the temperature and k_b is the Boltzmann constant, with the other terms as defined above.

A key issue in understanding conductivity in conjugated organic materials is to characterize those structural factors important in the hole transfer rates. For example, it has been demonstrated that the solid-state hole mobility in arylamines is related to the internal reorganization energy λ.[19] Since these are condensed-state systems, no solvent reorganization occurs during charge transfer, and the first, most tractable approximation ignores any environmental relaxation and changes in electronic polarization between an isolated system and the solid-state system. Although geometry-constraining nearest neighbor interactions are unlikely to be nonnegligible,[20] studies of isolated molecules are a necessary first step and their λ are a reasonable upper bound of the charge transport energetics involved. The present model, therefore, includes in λ only the internal reorganization energy of the isolated active oligomer or polymer. Unlike in solution, where solvent reorganization is often the dominant contributor,[21] the phonon-like modes of the solid-state environment are sufficiently stiff that local vibronic coupling should dominate. Hence, the reorganization energy for hole transfer in eq 1 can be expressed as follows:

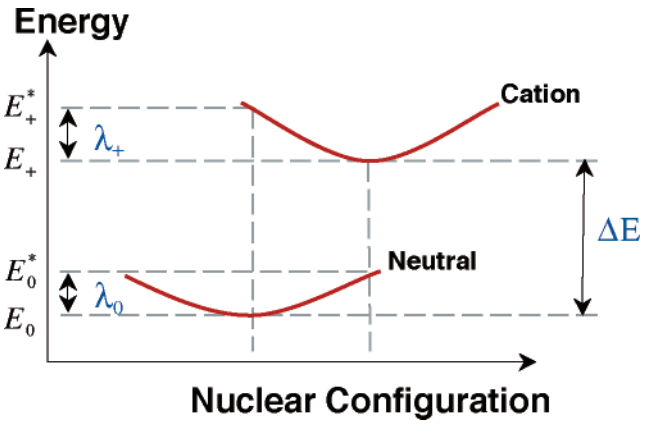

Figure 1. Internal reorganization energy for hole transfer as a function of various internal reorganization components $\lambda = \lambda_+ + \lambda_0$ and the adiabatic ionization energy (ΔE).

$$\lambda = \lambda_0 + \lambda_+ = (E_0^* - E_0) + (E_+^* - E_+) \qquad (3)$$

As illustrated in Figure 1, E_0 and E_+ represent the energies of the neutral and cation species in their lowest energy geometries, respectively, while E_0* and E_+* represent the energies of the neutral and cation species with the geometries of the cation and neutral species, respectively. This description holds as long as the potential energy surfaces are harmonic, and the λ_0 and λ_+ terms are close in energy.

A number of factors, including heteroatom identity, heterocycle substituents, and conjugation length, are known to be important in dictating the optical properties of conjugated organic oligomers and polymers, particularly optical band gaps[22−25] and bandwidths.[22] Characterizing reorganization energies in a similar manner would provide an assessment of the range of operative charge transfer rates and, using reported values for the electronic coupling matrix elements, would provide guidance for designing new, highly conductive materials. Furthermore, such an analysis would quantitatively assess relative contributions of bandwidth effects (from the electronic coupling matrix element) vs geometric reorganization effects (from the internal reorganization energies) in observed hole mobilities.

We present here a multidimensional, systematic investigation of the effects of molecular structure parameters such as

(10) (a) Brédas, J. L.; Calbert, J. P.; da Silva, D. A.; Cornil, J. *Proc. Natl. Acad. Sci. U.S.A.* **2002**, *99*, 5804. (b) Cornil, J.; Beljonne, D.; Calbert, J. P.; Brédas, J. L. *Adv. Mater.* **2001**, *13*, 1053.
(11) Hutchison, G. R.; Ratner, M. A.; Marks, T. J., submitted to *J. Am. Chem. Soc.*
(12) (a) Siriwong, K.; Voityuk, A. A.; Newton, M. D.; Rosch, N. *J. Phys. Chem. B* **2003**, *107*, 2595. (b) Blomgren, F.; Larsson, S.; Nelsen, S. F. *J. Comput. Chem.* **2001**, *22*, 655. (c) Newton, M. D. *Int. J. Quantum Chem.* **2000**, *77*, 255. (d) Nelsen, S. F.; Trieber, D. A.; Nagy, M. A.; Konradsson, A.; Halfen, D. T.; Splan, K. A.; Pladziewicz, J. R. *J. Am. Chem. Soc.* **2000**, *122*, 5940. (e) Nelsen, S. F.; Ismagilov, R. F.; Gentile, K. E.; Nagy, M. A.; Tran, H. Q.; Qu, Q.; Halfen, D. T.; Odegard, A. L.; Pladziewicz, J. R. *J. Am. Chem. Soc.* **1998**, *120*, 8230. (f) Jakobsen, S.; Mikkelsen, K. V.; Pedersen, S. U. *J. Phys. Chem.* **1996**, *100*, 7411. (g) Todd, M. D.; Mikkelsen, K. V. *Inorg. Chim. Acta* **1994**, *226*, 237.
(13) Blomgren, F.; Larsson, S. *Theor. Chem. Acc.* **2003**, *110*, 165.
(14) (a) Bixon, M.; Jortner, J. *Adv. Chem. Phys.* **1999**, *106*, 35. (b) Barbara, P. F.; Meyer, T. J.; Ratner, M. A. *J. Phys. Chem.* **1996**, *100*, 13148. (c) Marcus, R. A. *Rev. Mod. Phys.* **1993**, *65*, 599. (d) Newton, M. D.; Sutin, N. *Annu. Rev. Phys. Chem.* **1984**, *35*, 437. (e) Newton, M. D. *Adv. Chem. Phys.* **1999**, *106*, 303.
(15) Berlin, Y. A.; Hutchison, G. R.; Rempala, P.; Ratner, M. A.; Michl, J. *J. Phys. Chem. A* **2003**, *107*, 3970.
(16) Segal, D.; Nitzan, A.; Hanggi, P. *J. Chem. Phys.* **2003**, *119*, 6840.
(17) (a) Johansson, E.; Larsson, S. *Synth. Met.* **2004**, *144*, 183. (b) Larsson, S.; Klimkans, A.; Rodriguez-Monge, L.; Duskesas, G. *Theochem-J. Mol. Struct.* **1998**, *425*, 155. (c) Duskesas, G.; Larsson, S. *Theor. Chem. Acc.* **1997**, *97*, 110. (d) Rodriguez-Monge, L.; Larsson, S. *J. Chem. Phys.* **1996**, *105*, 7857. (e) Larsson, S.; Rodriguez-Monge, L. *Int. J. Quantum Chem.* **1996**, *58*, 517. (f) Silinsh, E. A.; Klimkans, A.; Larsson, S.; Capek, V. *Chem. Phys.* **1995**, *198*, 311. (g) Rodriguez-Monge, L.; Larsson, S. *J. Chem. Phys.* **1995**, *102*, 7106.
(18) (a) Marcus, R. A.; Eyring, H. *Annu. Rev. Phys. Chem.* **1964**, *15*, 155. (b) McConnell, H. M. *J. Chem. Phys.* **1961**, *35*, 508. (c) Hush, N. S. *J. Chem. Phys.* **1958**, *28*, 962. (d) Marcus, R. A. *J. Chem. Phys.* **1956**, *24*, 966.
(19) (a) Lin, B. C.; Cheng, C. P.; Lao, Z. P. M. *J. Phys. Chem. A* **2003**, *107*, 5241. (b) Malagoli, M.; Brédas, J. L. *Chem. Phys. Lett.* **2000**, *327*, 13. (c) Sakanoue, K.; Motoda, M.; Sugimoto, M.; Sakaki, S. *J. Phys. Chem. A* **1999**, *103*, 5551.
(20) Bromley, S. T.; Mas-Torrent, M.; Hadley, P.; Rovira, C. *J. Am. Chem. Soc.* **2004**, *126*, 6544.
(21) (a) Tavernier, H. L.; Fayer, M. D. *J. Chem. Phys.* **2001**, *114*, 4552. (b) Matyushov, D. V.; Voth, G. A. *J. Phys. Chem. A* **2000**, *104*, 6470. (c) Tavernier, H. L.; Kalashnikov, M. M.; Fayer, M. D. *J. Chem. Phys.* **2000**, *113*, 10191. (d) Raineri, F. O.; Friedman, H. L. *Adv. Chem. Phys.* **1999**, *107*, 81. (e) Matyushov, D. V.; Voth, G. A. *J. Phys. Chem. A* **1999**, *103*, 10981. (f) Kelley, A. M. *J. Phys. Chem. A* **1999**, *103*, 6891. (g) LeBard, D. N.; Lilichenko, M.; Matyushov, D. V.; Berlin, Y. A.; Ratner, M. A. *J. Phys. Chem. B* **2003**, *107*, 14509.
(22) Hutchison, G. R.; Zhao, Y. J.; Delley, B.; Freeman, A. J.; Ratner, M. A.; Marks, T. J. *Phys. Rev. B* **2003**, *68*, 035204.
(23) Cui, C. X.; Kertesz, M.; Jiang, Y. *J. Phys. Chem.* **1990**, *94*, 5172.
(24) Lee, Y. S.; Kertesz, M. *J. Chem. Phys.* **1988**, *88*, 2609.
(25) Hutchison, G. R.; Ratner, M. A.; Marks, T. J. *J. Phys. Chem. B*, in press.

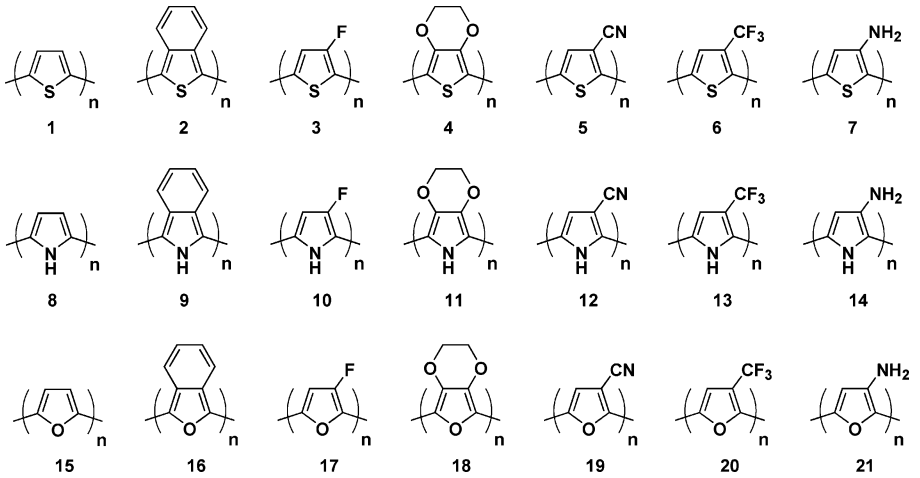

Figure 2. Structures used for multidimensional computational study. Note that a wide variety of substituents is used, including electron donors, electron acceptors, as well as commonly used isobenzo (**2**, **9**, **16**) and ethylenedioxy (**4**, **11**, **18**) substituents. In all cases, oligomer dimensions were varied from 2 to 6 monomer units ($n = 2-6$).

heteroatom identity, heterocycle substituent, and oligomer dimensions on the internal reorganization energies connecting the neutral and corresponding cations for a broad series of oligoheterocycles (Figure 2). These particular species were chosen for their diversity and because there are extensive experimental and theoretical databases.[26] We employ density functional methods (DFT) for computing the internal reorganization energies, as given by eq 3, and consider which structural factors are most important in dictating reorganization energies.

It will be seen that when neutral-cation pairs have greatly different inter-ring dihedral angles, torsional motion often accounts for a significant portion of the total reorganization energy. Consequently, we compute here the torsional profiles for all pairs studied (Figure 2) and consider which structural factors dominate these energetics. We compare the range of internal reorganization energies to the range of orbital splittings recently computed in oligothiophenes and other oligoheterocycles,[11] in the context of overall hole transfer rates. It will be seen that variations in internal reorganization energies, which have an exponential barrier (eq 2), dominate the changes in overall hole transfer rates as the molecular structures are varied. We compare this to experimental trends in hole mobilities and thermal transport activation barriers for various oligothiophenes and arylamines, and predict the temperature dependence of the intrinsic charge-transfer rate for the widely studied organic semiconductor sexithiophene.[27] We also consider the assumptions implicit in the charge-transfer model (eq 2) and the implications on the results presented here.

II. Computational Methods

To treat the interplay of oligomer length (measured as the number of monomer units), heteroatom, and heterocycle substituents completely, a total of 105 oligomers were studied in both neutral and cationic form. These encompassed oligomers having from 2 to 6 heterocyclic rings; substituted thiophenes, furans, and pyrroles; the parent unsubstituted compounds; and six different substituents, as indicated in Figure 2. The various substituents examined were chosen either as known oligothiophene or oligopyrrole substituents or for their established σ- and π-donating or withdrawing properties. The large number of species allows statistical analysis of the results, to minimize the effects of small random errors or computational inadequacies of DFT. Furthermore, since a wide range of molecules is studied, one can have confidence in estimates of the consequences of each principal structural modification.

Full geometry optimization for each molecule in the neutral and cationic states was completed using the Q-Chem 2.0 program[28] with the B3LYP hybrid density functional[29] and the 6-31G* basis set. No symmetry constraints were enforced, and in all cases, several conformations were considered in attempting to locate the global minimum energy geometry. All open-shell calculations were performed using unrestricted methods (UDFT), and spin contamination in the radical cation species was found to be very small ($\langle S^2 \rangle \leq 0.77$; less than 3% from the exact expected value, 0.75). The internal harmonic reorganization energies were then calculated from these relaxed geometries, as given by eq 3, and summarized in Table 1, as were the adiabatic ionization potentials of each species, given by the following:

$$\Delta E = E_+ - E_0 \tag{4}$$

Torsional profiles were computed for each dimer by increasing

(26) (a) Seixas de Melo, J.; Elisei, F.; Gartner, C.; Gaetano Aloisi, G.; Becker, R. S. *J. Phys. Chem. A* **2000**, *104*, 6907. (b) Fichou, D. *Handbook of Oligo- and Polythiophenes*; Wiley-VCH: Weinheim; New York, **1999**. (c) Cornil, J.; Beljonne, D.; Brédas, J. L. In *Electronic Materials: The Oligomer Approach*; Wiley-VCH: Weinheim, **1998**; pp 432. (d) Bäuerle, P. In *Electronic Materials: The Oligomer Approach*; Müllen, K., Egner, G., Eds.; Wiley-VCH: Weinheim, 1998; pp 105. (e) Groenendaal, L.; Meijer, E. W.; Vekemans, J. A. J. M. In *Electronic Materials: The Oligomer Approach*; Müllen, K., Egner, G., Eds.; Wiley-VCH: Weinheim, **1998**; pp 235. (f) McCullough, R. D. *Adv. Mater.* **1998**, *10*, 93. (g) Roncali, J. In *Handbook of Conducting Polymers*, 2nd ed.; Skotheim, T. A., Elsebaumer, R. L., Reynolds, J. R., Eds.; Marcel Dekker: New York, 1998; pp 311. (h) Glenis, S.; Benz, M.; Legoff, E.; Schindler, J. L.; Kannewurf, C. R.; Kanatzidis, M. G. *J. Am. Chem. Soc.* **1993**, *115*, 12519. (i) Kauffmann, T.; Lexy, H. *Chem. Ber.* **1981**, *114*, 3667.

(27) Communicated in part at: (a) Excited-State Processes in Electronic and Bio-Nanomaterials, Los Alamos, August 11−16, 2003. (b) ACS Prospectives Symposium "Organic Thin Film Electronics," Miami, Jan. 25−28, 2004. (c) The 227th National Meeting of the ACS, Annaheim CA.; Facchetti, A.; Hutchison, G.; Yoon, M.-H.; Letizia, J.; Ratner, M. A.; Marks, T. J. Polymer Preprints, **2004**, *45*, 185−186. (d) Sixth International Symposium on Functional π-Electron Systems, Ithaca, NY, June 14−18, 2004.

(28) Kong, J.; White, C. A.; Krylov, A. I.; Sherrill, C. D.; Adamson, R. D.; Furlani, T. R.; Lee, M. S.; Lee, A. M.; Gwaltney, S. R.; Adams, T. R.; Ochsenfeld, C.; Gilbert, A. T. B.; Kedziora, G. S.; Rassolov, V. A.; Maurice, D. R.; Nair, N.; Shao, Y.; Besley, N. A.; Maslen, P. E.; Dombroski, J. P.; Dachsel, H.; Zhang, W. M.; Korambath, P. P.; Baker, J.; Byrd, E. F. C.; Van Voorhis, T.; Oumi, M.; Hirata, S.; Hsu, C. P.; Ishikawa, N.; Florian, J.; Warshel, A.; Johnson, B. G.; Gill, P. M. W.; Head-Gordon, M.; Pople, J. A. *J. Comput. Chem.* **2000**, *21*, 1532.

Table 1. Computed Internal Reorganization Energies (λ, in eV) for Hole Transfer (eq 3) for Each of the Oligoheterocycles of Figure 2

series	monomer units	λ	series	monomer units	λ	series	monomer units	λ
1	2	0.365	**8**	2	0.353	**15**	2	0.315
	3	0.321		3	0.312		3	0.292
	4	0.293		4	0.281		4	0.271
	5	0.272		5	0.253		5	0.252
	6	0.253		6	0.228		6	0.234
2	2	0.210	**9**	2	0.295	**16**	2	0.195
	3	0.202		3	0.330		3	0.189
	4	0.522		4	0.287		4	0.191
	5	0.428		5	0.265		5	0.190
	6	0.510		6	0.334		6	0.183
3	2	0.409	**10**	2	0.413	**17**	2	0.388
	3	0.357		3	0.360		3	0.349
	4	0.327		4	0.323		4	0.320
	5	0.304		5	0.293		5	0.301
	6	0.286		6	0.266		6	0.282
4	2	0.440	**11**	2	0.439	**18**	2	0.448
	3	0.385		3	0.396		3	0.397
	4	0.349		4	0.356		4	0.356
	5	0.321		5	0.325		5	0.330
	6	0.296		6	0.298		6	0.305
5	2	0.325	**12**	2	0.317	**19**	2	0.279
	3	0.288		3	0.279		3	0.257
	4	0.263		4	0.251		4	0.241
	5	0.241		5	0.224		5	0.222
	6	0.221		6	0.201		6	0.202
6	2	0.668	**13**	2	0.567	**20**	2	0.440
	3	0.639		3	0.476		3	0.390
	4	0.550		4	0.407		4	0.353
	5	0.535		5	0.370		5	0.325
	6	0.475		6	0.335		6	0.288
7	2	0.658	**14**	2	0.677	**21**	2	0.710
	3	0.554		3	0.528		3	0.620
	4	0.505		4	0.430		4	0.534
	5	0.487		5	0.394		5	0.493
	6	0.431		6	0.399		6	0.465

the inter-ring dihedral angle in 15° increments. Previous studies have demonstrated that electron correlation is important in computing λ,[30] and DFT methods generally give both reorganization energies comparable to those from second-order Møller−Plesset (MP2) calculations,[15] (slightly lower than that measured experimentally from photoelectron spectroscopy for fused-ring aromatic molecules),[31] and reasonable estimates of the inter-ring torsional barriers in conjugated organic oligomers.[32]

All statistical analyses, including multifactor analysis of variance (ANOVA) and multivariate regressions, were performed with the *R* statistical package, version 1.7.1.[33] The principal structural factors considered were the heteroatom, substituent, charge, and oligomer size. ANOVA was performed on the entire data set, including principal structural factors, and two- and three-way interactions, on the calculated internal reorganization energies. Significant effects were taken to be those in the ANOVA model with confidence levels of 99% or higher, as indicated in Table 2, and were used to establish multivariate linear regressions for each of the responses mentioned above. A separate analysis was performed using geometric measures of C−C bond length alternation along the oligomer chain, and the average inter-ring dihedral angle of the optimized oligomers, as described below.

Table 2. Linear Regression Results for Internal Reorganization Energies (λ) of the Oligoheterocycles in Figure 2 as a Function of the Square Root of the Number of Monomer Units N (i.e., $\lambda = C_0 + C_1\sqrt{N}$), with the R^2 Values of the Fits Indicated in Column 4[a]

molecule	intercept (C_0 in eV)	slope C_1 in eV·(mon. units)$^{-1/2}$	R^2
1	0.511	−0.107	0.989
2	−0.263	0.324	0.702
3	0.567	−0.117	0.981
4	0.629	−0.138	0.992
5	0.463	−0.099	0.997
6	0.946	−0.189	0.958
7	0.930	−0.205	0.958
8	0.522	−0.120	0.999
9	0.295	0.003	0.002
10	0.608	−0.141	0.996
11	0.633	−0.137	0.999
12	0.474	−0.112	0.999
13	0.871	−0.224	0.982
14	1.028	−0.276	0.884
15	0.427	−0.078	0.999
16	0.207	−0.009	0.688
17	0.528	−0.102	0.992
18	0.639	−0.138	0.993
19	0.384	−0.073	0.993
20	0.641	−0.143	0.997
21	1.041	−0.242	0.976

[a] Note that the molecules showing little or no variability with oligomer length include series **2**, **9**, and **16**.

III. Results and Discussion

We first consider the effects of oligomer length on computed λ for all-*trans*-oligoenes, and then how these effects differ from the trends observed in the heterocyclic oligomers. Next, we discuss building statistical models for interpreting the results, including determining the most important λ-governing structural factors to include, as well as the chemical and physical meaning of the resulting statistics. We then compare λ to neutral and cation time-dependent density functional theory (TDDFT) excitation energies computed for these species.[25] From these results, we consider the consequences for prospective conductive materials which are also optically transparent, and compare the computed bandwidths for oligothiophenes and other organic solids.[11] The latter results demonstrate that internal reorganization energy changes dominate trends in hole transfer rates in such materials.

A. Oligomer Length Effects on λ. Generally, we find that the internal reorganization energies of each oligomer family decrease as the oligomer degree of polymerization increases, due to the greater positive charge delocalization in longer oligomers. In the case of a self-localized polaron, this trend will eventually level off, as the reorganization energy beyond the localization length of the polaron will remain constant, as illustrated in Figure 3. If an oligomer is longer than the localization length, then the regions outside the polaron will not change geometry and hence will not contribute to λ. Using

(29) (a) Becke, A. D. *J. Chem. Phys.* **1993**, *98*, 5648. (b) Lee, C.; Yang, W.; Parr, R. G. *Phys. Rev. B* **1988**, *37*, 785.
(30) (a) Klimkans, A.; Larsson, S. *Int. J. Quantum Chem.* **2000**, *77*, 211. (b) Klimkans, A.; Larsson, S. *Chem. Phys.* **1994**, *189*, 25.
(31) (a) Gruhn, N. E.; da Silva, D. A.; Bill, T. G.; Malagoli, M.; Coropceanu, V.; Kahn, A.; Brédas, J. L. *J. Am. Chem. Soc.* **2002**, *124*, 7918. (b) Amashukeli, X.; Winkler, J. R.; Gray, H. B.; Gruhn, N. E.; Lichtenberger, D. L. *J. Phys. Chem. A* **2002**, *106*, 7593.
(32) (a) Grein, F. *THEOCHEM* **2003**, *624*, 23. (b) Hehre, W. J. *A Guide to Molecular Mechanics and Quantum Chemical Calculations*; Wavefunction, Inc.: Irvine, CA, 2003. (c) Grein, F. *J. Phys. Chem. A* **2002**, *106*, 3823. (d) Mohamed, A. A. *Int. J. Quantum Chem.* **2000**, *79*, 367. (e) Karpfen, A.; Choi, C. H.; Kertesz, M. *J. Phys. Chem. A* **1997**, *101*, 7426.
(33) Ihaka, R.; Gentleman, R. *J. Comput. Graph. Statist.* **1996**, *5*, 299.

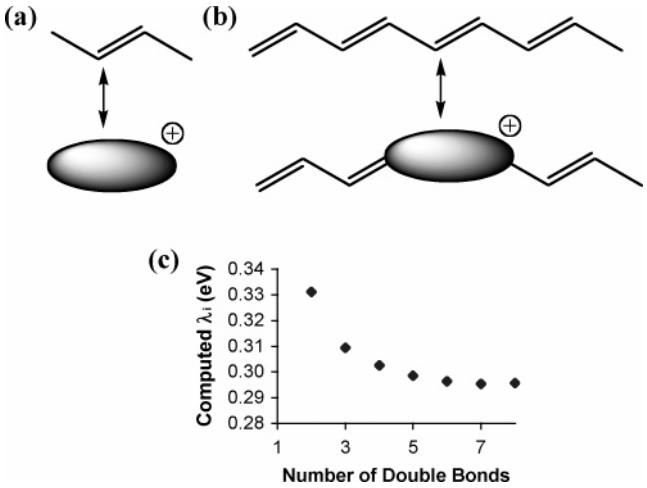

Figure 3. Illustration of the effect of localized polaron formation on the internal reorganization energy of oligoenes as a function of oligomer/polymer length. At small lengths, (a) the polaron delocalizes over entire chain, causing large geometric reorganization. At longer lengths, (b) the localized polaron forces geometric changes only over a portion of the chain. Beyond the length of this finite polaron, the internal reorganization energy saturates, (c) as computed for all-*trans*-oligoenes of increasing length.

the DFT methods described above, this behavior is indeed observed for a series of all-*trans*-oligoenes of increasing length as illustrated in Figure 3c. However, there is little to suggest functional scaling of the reorganization energies with oligomer length before this polaron localization length is reached, in contrast to the well-established approximate "1/*N*" relationship between band gap and length in conjugated oligomers of short length, observed both experimentally and theoretically.[22,34]

To model accurately a nonlinear variable in a linear statistical model (as is the case here), it is necessary to transform the data in such a manner as to identify a linear correlation. As noted above, the band gaps and optical absorption properties of short oligomers do not vary linearly with the number of monomer units, but rather with 1/*N*. Hence, even an empirical relationship between oligomer length and internal reorganization energy is needed before proceeding with further statistical analysis. As shown in Figure 4a, the internal reorganization energies computed for the parent (unsubstituted) oligothiophenes, oligopyrroles, and oligofurans, do not exhibit the self-localized polaron effects mentioned above for the lengths studied (2−12 monomer units). Furthermore, the internal reorganization energies do not scale linearly with 1/*N* (Figure 4b), instead exhibiting an inverse correlation with the square-root of the number of monomer units (Figure 4c). This empirical $-c\sqrt{N}$ scaling law observed for the parent oligoheterocycles also fits most of the other oligomer families studied, as summarized in Table 2. The three series that do not exhibit good fits, **2**, **9**, and **16**, also do not show appreciable length dependence of reorganization energies, as discussed below.

B. Effects of C−C π-Backbone Bond Length Alternation and Average Inter-ring Dihedral Angle on λ. Since the internal reorganization energy is a measure of the geometric distortion as a result of charge transfer, an obvious model would consider the computed λ as a function of changes in molecular geometry. Theoretical studies on conjugated oligomers and

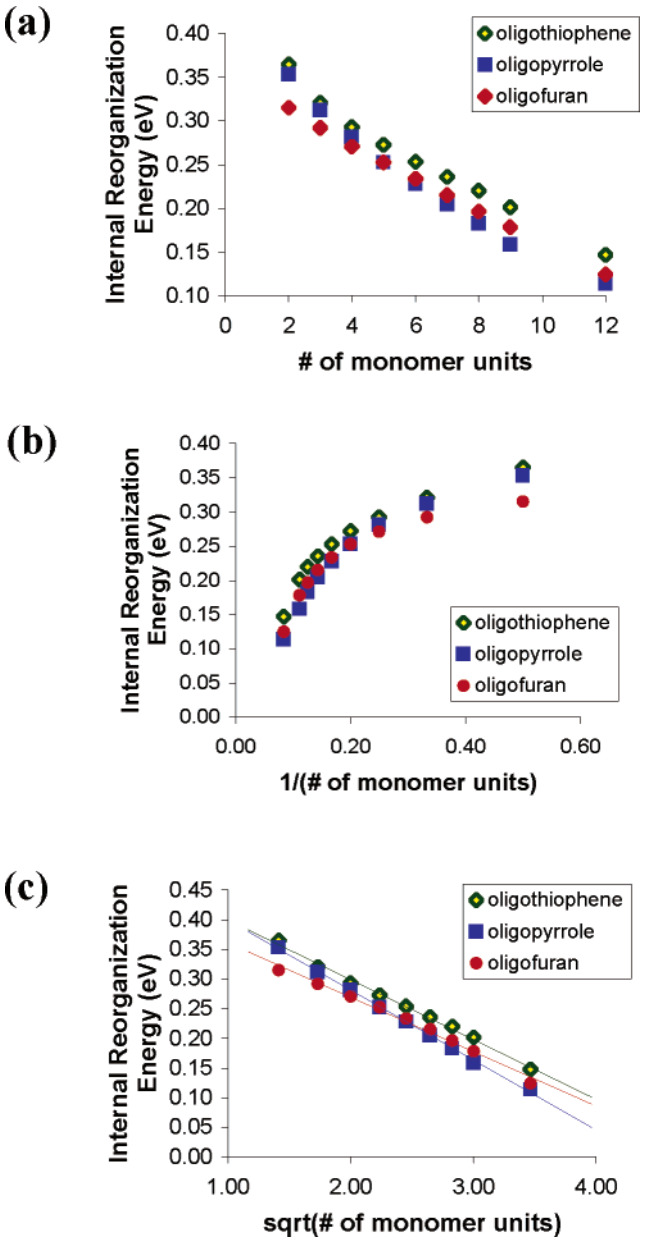

Figure 4. Scaling of the internal reorganization energy of oligothiophenes **1**, oligopyrroles **8**, and oligofurans **15** having from 2 to 12 monomer units, plotted relative to the following: (a) the number of monomer units (*N*), (b) 1/*N*, showing a nonlinear correlation, and (c) the $\sqrt{N}$, indicating a linear correlation for all three sets of oligomers.

polymers frequently consider π-backbone bond length alternation, since these bonds often undergo dramatic changes in length in response to changes in electronic state.[13,24,35] Previous research on internal reorganization energies also indicates that dihedral angle changes are often significant contributors to λ.[15] Consequently, the first model for computed reorganization energies considers λ as a function of a linear combination of the changes in bond length alternation (ΔL) and average inter-

(34) (a) de Melo, J. S.; Silva, L. M.; Arnaut, L. G.; Becker, R. S. *J. Chem. Phys.* **1999**, *111*, 5427. (b) Taubmann, G. *J. Chem. Educ.* **1992**, *69*, 96. (c) Kuhn, H. *J. Chem. Phys.* **1949**, *17*, 1198.

(35) (a) Gorman, C. B.; Marder, S. R. *Chem. Mater.* **1995**, *7*, 215. (b) Bourhill, G.; Brédas, J.-L.; Cheng, L.-T.; Marder, S. R.; Meyers, F.; Perry, J. W.; Tiemann, B. G. *J. Am. Chem. Soc.* **1994**, *116*, 2619. (c) Meyers, F.; Marder, S. R.; Pierce, B. M.; Brédas, J. L. *J. Am. Chem. Soc.* **1994**, *116*, 10703. (d) Marder, S. R.; Perry, J. W.; Bourhill, G.; Gorman, C. B.; Tiemann, B. G.; Mansour, K. *Science* **1993**, *261*, 186. (e) Marder, S. R.; Perry, J. W.; Tiemann, B. G.; Gorman, C. B.; Gilmour, S.; Biddle, S. L.; Bourhill, G. *J. Am. Chem. Soc.* **1993**, *115*, 2524.

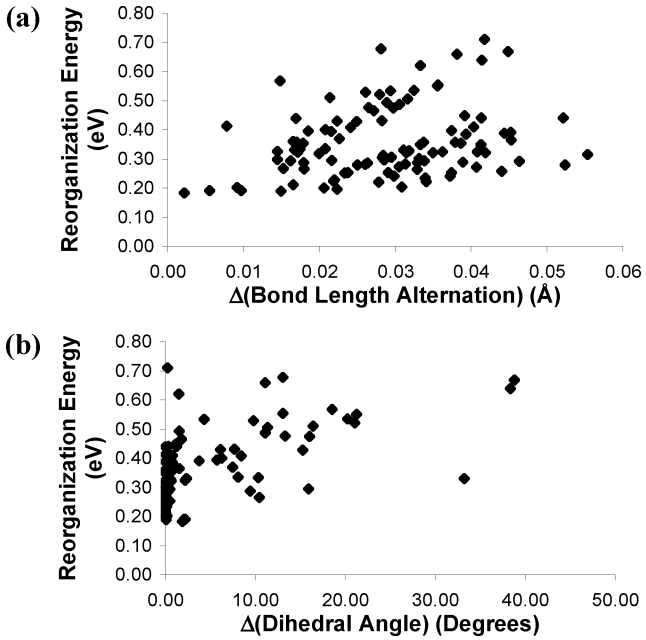

Figure 5. Comparison of the computed internal reorganization energies of all oligomers in Figure 2 to the following: (a) change in C−C π-backbone bond length alternation between the neutral and cation species and (b) change in average inter-ring dihedral angle between the neutral and cation species. Since many of the oligomers prefer a planar conformation for both neutral and cation species, (b) shows few oligomers with large torsional changes.

ring dihedral angle (ΔD) on oxidation from the neutral to the corresponding monocationic oligomer

$$\lambda = C_0 + C_1\Delta L + C_2\Delta D \quad (5)$$

where C_0, C_1, and C_2 are the coefficients from the multivariate least-squares fit. While Figure 5 suggests that taken separately, changes in bond length alternation and average inter-ring dihedral angle do not have a significant correlation with the computed λ, Figure 6a illustrates slightly greater effectiveness of the two-factor model in eq 5. This result suggests that some species may exhibit smaller changes in dihedral angle but larger changes in bond lengths and vice-versa. However, the relatively low R^2 value indicates that the majority of the variation in computed reorganization energies is not exclusively due to geometric distortions in either bond lengths or inter-ring dihedral angles alone.

C. Heteroatom and Substitutent Effects on λ. There are, of course, other modes of geometric distortion in addition to those involving the C−C π-backbone and/or inter-ring dihedral angles, and large geometric distortions of any sort do not necessarily imply large reorganization energies since the relevant potential energy surfaces may be very flat. Consequently, a second approach to understanding the trends in reorganization energies is to model λ as a function of oligomer length, heteroatom, and heterocycle substituents. Since the changes in geometry, such as bond length alternation and dihedral angle, can also be described as implicit functions of these structural factors, only the three "principal factors" are explicitly included in this model:

$$\lambda = C_0 + C_1\sqrt{N} + C_2(\text{Heteroatom}) + C_3(\text{Substituent}) + C_4(\text{Charge}) \quad (6)$$

As illustrated in Figure 6b, the fit is now significantly better, with $R^2 = 0.736$, likely because this model implicitly considers the energy required to induce a geometric distortion, as well as other modes of distortion, such as nonbackbone bond-stretching. However, the ANOVA results in Table 3 and the R^2 value suggest that second-order interactions are important (i.e., the effects of oligomer length, heteroatom, and heterocycle substitutent are *not* strictly independent). Including the second-order interactions produces the "complete model"

$$\lambda = C_0 + C_1\sqrt{N} + C_2(\text{Heteroatom}) + C_3(\text{Substituent}) + C_4(\sqrt{N}\bullet\text{Heteroatom}) + C_5(\sqrt{N}\bullet\text{Substituent}) + C_6(\text{Heteroatom}\bullet\text{Substituent}) \quad (7)$$

where the various C_n parameters are fit by the multivariate regression and the $\bullet$ is taken as a combination of two or more principal factors (e.g., heteroatom•substituent might be inserted for heteroatom = S (thiophene) *and* substituent = isobenzo). In the case of categorical factors, such as heteroatom identity and substituent, the appropriate additive factor is looked up based on the particular species, but for the continuous $\sqrt{N}$ factor representing oligomer length, $\sqrt{N}$ is multiplied by the appropriate additive factor. This model is illustrated in Figure 6c and derived parameters are summarized in Table 4—it is significantly more accurate in describing the computed reorganization energies as a function of structural motif than the principal factors model. The average absolute error in this final model is only 0.017 eV (vs 0.043 eV for the principal factors model alone). As an example of using eq 7, the predicted λ for a tetramer of series 20 from Table 4 would be as follows:

$$\lambda(\text{in eV}) = 0.433 - 0.067\sqrt{4} + 0.043(\text{furan}) + 0.437(\text{trifluoromethyl}) + -0.036(\sqrt{4}\cdot\text{furan}) - 0.084(\sqrt{4}\cdot\text{trifluoromethyl}) + -0.186(\text{furan}\cdot\text{trifluoromethyl}) \quad (8)$$

which yields λ of 0.353 eV, identical to the DFT-computed λ of 0.353 eV.

Several trends emerge from the data in Table 4. As discussed above, reorganization energies decrease with increasing oligomer length (decrement proportional to $\sqrt{N}$), although the second-order interactions indicate that oligofurans and oligopyrroles yield greater decreases in reorganization energies at greater oligomer lengths, perhaps because the smaller size of the heterocyclic rings allows these oligomers to assume more planar conformations, on average. The structures with ethylenedioxy, trifluoromethyl, and amino substituents all exhibit significantly higher computed reorganization energies, probably due to torsional effects to be discussed below. The isobenzo-substituted oligomers (i.e., series **2**, **9**, and **16**) all exhibit significantly smaller computed reorganization energies which have minimal oligomer length dependence (evident in the low R^2 values and small or negative C_1 coefficients from the fits to oligomer length in Table 2), likely because the increased delocalization into the fused benzene ring diminishes geometric differences between neutral and cationic oligomers, and much of the remaining reorganization energies result from torsional changes. The striking lack of oligomer length dependence in the case of the isobenzo substituent reflects a balance between the (small)

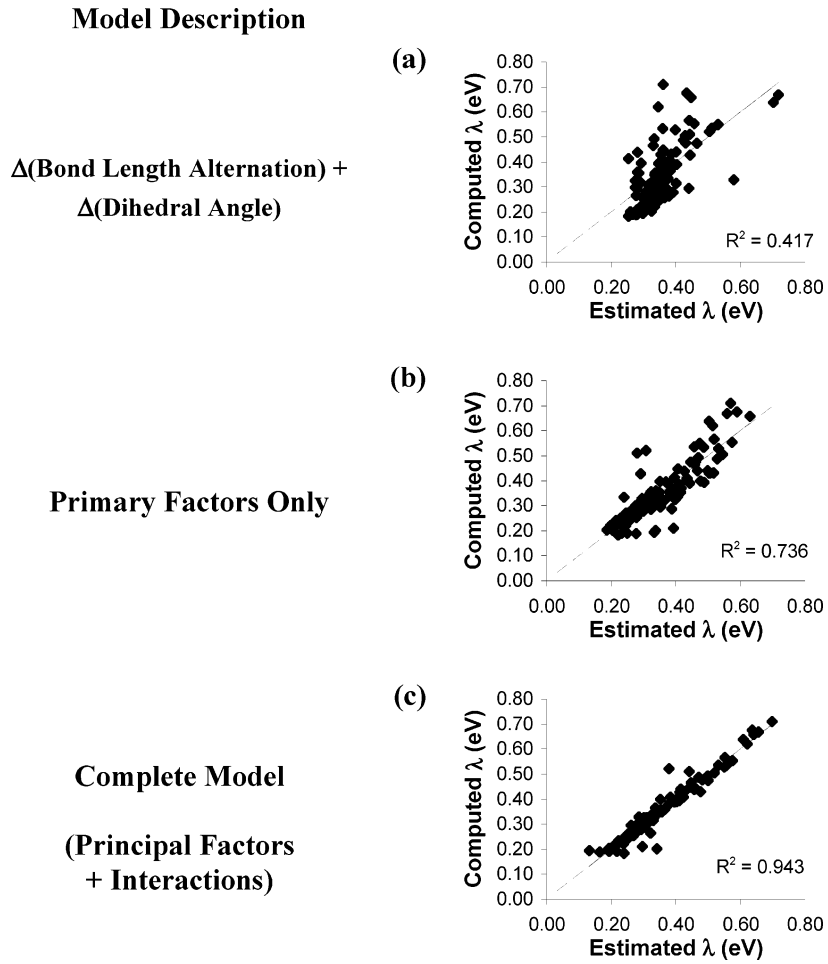

Figure 6. Comparison of various statistical models for estimating the internal reorganization energy (λ) for all oligomers in Figure 2, to the computed values, including: (a) only bond length alternation and dihedral angle factors, (b) oligomer length, heteroatom, and heterocycle substituents factors, but no interactions, and (c) the complete model with second-order interactions.

Table 3. Three-Way ANOVA Analysis of the Principal Factors and Interactions for Computed Adiabatic Ionization Energy (ΔE) and Internal Reorganization Energy (λ) for All Oligomers in Figure 2[a]

effect	ΔE	λ.
principal factors		
oligomer length	X	X
heteroatom	X	X
substituent	X	X
interactions (2^{nd} order)		
oligomer length:heteroatom	X	X
oligomer length:substituent	X	X
heteroatom:substituent	X	X
interactions (3^{rd} order)		
oligomer length:heteroatom:substituent		X

[a] Filled cells (X) indicate factors which are statistically significant for that variable with a 99% confidence level. This compilation summarizes which factors are important in predicting the variation in ΔE or λ and demonstrates which factors and interactions should be used for models. Note that for the scaling of ΔE with oligomer length, the $1/N$ trend was used (as typically used for HOMO/LUMO energies and HOMO−LUMO gaps), while for the scaling of λ with oligomer length, the empirical $\sqrt{N}$ trend was used, as discussed in the text.

decrease in reorganization energy with increased length due to increased conjugation and the additional torsional changes required to planarize additional monomer units as the oligomer degree of polymerization increases.

Table 4 also includes those factors important for the adiabatic ionization energy (ΔE), calculated from eq 4, although as illustrated in Figure 7, this parameter is highly correlated with the DFT-computed HOMO energies of the neutral species (E_{HOMO}), having a linear regression of

$$E_{HOMO} = -0.850(\Delta E) + 0.257 \text{ eV} \qquad (9)$$

where both E_{HOMO} and ΔE are in eV. The average absolute error in this relationship is only 0.169 eV, so it is reasonable to suggest that the B3LYP functional used in these computations produces similar accuracy in computed ionization potentials either from the HOMO eigenvalue/orbital energy or from the ΔSCF method, even though Koopmans' theorem is not strictly valid for DFT methods, since Kohn−Sham eigenvalues cannot be formally interpreted as orbital energies for excited states.[36]

D. Neutral and Cation Inter-ring Torsional Profiles. To estimate the contribution of rotational barriers to total internal λ, torsional potential energy curves were computed for the dimers of each neutral and cationic pair in Figure 2, as described above. These torsional profiles are summarized in Table 5, which gives the inter-ring dihedral angles of lowest and highest potential energy and the rotational barrier for the species. Each potential energy curve was fit by a least-squares spline curve and consequently, the extremal angles do not strictly lie on the 15° rotations considered by the DFT calculations. It is found that the monocations typically have significantly higher rota-

(36) (a) Stowasser, R.; Hoffmann, R. *J. Am. Chem. Soc.* **1999**, *121*, 3414. (b) Godby, R. W.; Schluter, M.; Sham, L. J. *Phys. Rev. B* **1988**, *37*, 10159.

Table 4. Overall Linear Models, Constructed from the Principal Factors and All Second-Order Interactions for Computed Adiabatic Ionization Energies (ΔE) and Internal Reorganization Energies (λ) for All Oligomers in Figure 2[a]

effect	ΔE	λ
intercept	5.092	0.433
principal factors		
oligomer length	4.048 eV· (monomer units)	−0.067 eV· (monomer units)$^{-1/2}$
heteroatom (furan)	−0.202	0.043
heteroatom (pyrrole)	−0.765	0.118
substituent (isobenzo)	−0.678	−0.335
substituent (fluoro)	0.246	0.072
substituent (ethylenedioxy)	−1.064	0.128
substituent (cyano)	1.404	−0.047
substituent (trifluoromethyl)	1.047	0.437
substituent (amino)	−0.652	0.500
interactions (2nd order)		
length:heteroatom (furan)	0.316 eV· (monomer units)	−0.036 eV· (monomer units)$^{-1/2}$
length:heteroatom (pyrrole)	0.087 eV· (monomer units)	−0.068 eV· (monomer units)$^{-1/2}$
length:substituent (isobenzo)	−0.657 eV· (monomer units)	0.208 eV· (monomer units)$^{-1/2}$
length:substituent (fluoro)	−0.077 eV· (monomer units)	−0.018 eV· (monomer units)$^{-1/2}$
length:substituent (ethylenedioxy)	0.429 eV· (monomer units)	−0.036 eV· (monomer units)$^{-1/2}$
length:substituent (cyano)	−1.028 eV· (monomer units)	0.007 eV· (monomer units)$^{-1/2}$
length:substituent (trifluoromethyl)	−0.775 eV· (monomer units)	−0.084 eV· (monomer units)$^{-1/2}$
length:substituent (amino)	−0.461 eV· (monomer units)	−0.139 V·set (monomer units)$^{-1/2}$
heteroatom (furan): substituent (isonaphthyl)	−0.179	−0.157
heteroatom (pyrrole): substituent (isonaphthyl)	0.279	−0.057
heteroatom (furan): substituent (fluoro)	0.007	0.019
heteroatom (pyrrole): substituent (fluoro)	0.017	0.010
heteroatom (furan): substituent (ethylenedioxy)	−0.051	0.037
heteroatom (pyrrole): substituent (ethylenedioxy)	0.143	0.020
heteroatom (furan): substituent (cyano)	0.154	0.001
heteroatom (pyrrole): substituent (cyano)	0.220	0.002
heteroatom (furan): substituent (trifluoromethyl)	0.022	−0.186
heteroatom (pyrrole): substituent (trifluoromethyl)	0.097	−0.127
heteroatom (furan): substituent (amino)	−0.179	0.065
heteroatom (pyrrole): substituent (amino)	0.163	−0.026

[a] Categorical effects (discrete set of choices such as heteroatom or substituent) are relative to the neutral oligothiophene parent (compound 1). Note that for the scaling of ΔE with oligomer length, the $1/N$ trend was used (as typically used for HOMO/LUMO energies and HOMO−LUMO gap), while for the scaling of λ with oligomer length, the empirical $\sqrt{N}$ trend was used, as discussed in the text. Units are in eV, except where indicated.

tional barriers than do the corresponding neutral oligomers, and the average barrier is almost 20 kcal/mol higher (27.8 kcal/mol avg. vs 8.72 kcal/mol avg., respectively). This higher rotational barrier illustrates the energetic penalty for breaking π-conjugation in the cationic oligomers. The torsional profiles reflect a balance between two effects, the stabilizing C−C π-bond conjugation and destabilizing steric effects of eclipsing interactions. Breaking π-conjugation in cationic oligomers forces the positive charge onto a smaller effective conjugated unit, and this effect appears to dominate, judging from the larger

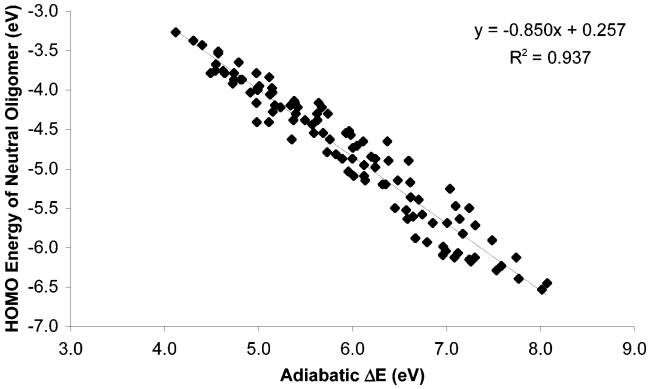

Figure 7. Correlation of the computed adiabatic ionization potential ΔE connecting neutral and cation optimized geometries for all oligomers in Figure 2, as indicated in Figure 1, with the corresponding HOMO energy computed for the corresponding neutral oligomer.

computed rotational barriers, and also because all oligomers except $\mathbf{2}^+$ exhibit the highest relative energies at dihedral angles approaching 90°. In contrast, the five neutral species exhibiting the largest rotational barriers (**2**, **4**, **9**, **11**, and **16**) exhibit the greatest relative energies at dihedral angles of 0°, implying that the largest contributions to the rotational barriers in the neutral species derive from steric interactions. Notably, these species all have isobenzo or ethylenedioxy substituents, which experience close nonbonding interactions in the *cisoid* conformation at dihedral angles of 0°.

Comparing dihedral angles at the energetic minima for corresponding neutral vs cationic oligomers, we find that series **1**, **2**, **5**, **6**, **7**, **8**, **9**, **13**, and **14** all have minima at significantly different dihedral angles. Figure 8 illustrates the torsional profiles for **6** and **9**, showing the different minima for the neutral and monocation oligomers. In both cases, the contribution of this torsional reorganization (given by the energy differences between the torsional profiles at the respective minima) to the overall λ for the species (cf., Figure 1) is significant, comprising 57% and 31% of the total λ for **6** and **9**, respectively. This large contribution illustrates that reduction of the heterocycle substituent steric bulk or other strategies to maintain the same inter-ring dihedral angle between neutral and cation states should significantly reduce the internal reorganization energy.

Torsional profile differences also explain some of the trends observed in reorganization energies. Of the 9 species exhibiting significant energetic differences between the minimum dihedral angles in neutral vs cation structures, four are pyrroles, a trend likely contributing to the higher reorganization energies computed for the pyrrole oligomers. Also, oligomers having electron-withdrawing trifluoromethyl and electron-releasing amino substituents, which show the greatest computed reorganization energies, comprise 4 of the 9, illustrating that the large contribution to the overall λ from torsional changes observed in Figure 8a for oligomer **6** is a general trend for such substituents. The relatively large sizes of the trifluoromethyl and amino groups enforce twisted conformations in oligomers of series **6**, **7**, and **13**, evident in the large inter-ring dihedral angles; all three oligomers distort to more planar geometries upon oxidation due to the large penalty for breaking π-conjugation in the cationic oligomers.

E. Comparisons of Internal Reorganization Energies to Computed TDDFT Optical Excitation Energies. Optically

Table 5. Angles of Highest and Lowest Computed Total Energies for Variation of the Interring Dihedral Angle in the Oligoheterocycle Dimers of Figure 2, as Well as Computed Rotational Barriers between These Two Extrema[a]

species	angle at energetic maxima (deg)	angle at energetic minimum (deg)	rotational barrier (kcal/mol)
1	89.1	159.5	2.82
2	0.0	138.8	43.62
3	86.9	179.2	3.57
4	0.0	179.0	12.18
5	88.7	169.2	2.95
6	14.7	138.2	5.67
7	11.6	149.9	4.69
8	81.1	152.6	3.49
9	0.0	144.2	21.32
10	0.0	180.0	5.33
11	0.0	179.7	11.40
12	78.5	180.0	7.28
13	0.0	153.9	7.21
14	80.2	179.6	9.71
15	92.7	179.8	5.72
16	0.0	180.0	10.59
17	92.7	179.9	4.36
18	91.7	178.9	2.97
19	91.6	180.0	5.99
20	94.4	178.7	5.49
21	91.4	179.7	6.72
$\mathbf{1}^+$	89.9	179.9	25.63
$\mathbf{2}^+$	0.0	167.4	38.46
$\mathbf{3}^+$	90.0	180.0	25.56
$\mathbf{4}^+$	90.1	179.3	27.49
$\mathbf{5}^+$	90.0	180.0	27.08
$\mathbf{6}^+$	89.7	177.1	24.56
$\mathbf{7}^+$	88.9	161.8	16.77
$\mathbf{8}^+$	89.7	180.0	26.64
$\mathbf{9}^+$	89.1	161.7	21.98
$\mathbf{10}^+$	89.8	180.0	28.84
$\mathbf{11}^+$	90.0	179.7	32.29
$\mathbf{12}^+$	89.6	180.0	28.59
$\mathbf{13}^+$	89.7	172.9	29.64
$\mathbf{14}^+$	87.3	165.9	23.34
$\mathbf{15}^+$	90.0	180.0	30.92
$\mathbf{16}^+$	90.1	180.0	29.61
$\mathbf{17}^+$	90.0	180.0	29.68
$\mathbf{18}^+$	89.4	177.8	29.06
$\mathbf{19}^+$	90.0	180.0	29.21
$\mathbf{20}^+$	90.1	179.9	30.18
$\mathbf{21}^+$	90.3	180.0	27.11

[a] Angles were computed from least-squares spline fitting to the potential energy curve.

Transparent Conductors. A recent computational study of the structure-dependent optical properties of the present heterocyclic oligomers predicted vertical optical band gaps for both neutral and monocationic states using TDDFT and ZINDO/CIS.[25] Consequently, it is possible to compare the computed optical absorption energies of these structures to the computed internal reorganization energies. We find for the oligomers studied here, that there is no obvious correlation (Figure 9) between the computed optical excitation energies for either neutral or monocation species and the corresponding internal reorganization energies. One reason for this lack of correlation is the distinct difference in importance of torsional effects in determining optical excitation energies and the internal reorganization energies for these same species. As outlined above, the change in energy accompanying change in dihedral angles between corresponding neutral and monocation species is often a significant contributor to λ. This is in dramatic contrast to the effects important in optical excitations, where we find that the bond length alternation and average dihedral angles barely express 10% of the variance in the computed TDDFT and ZINDO/CIS optical excitation energies.[25]

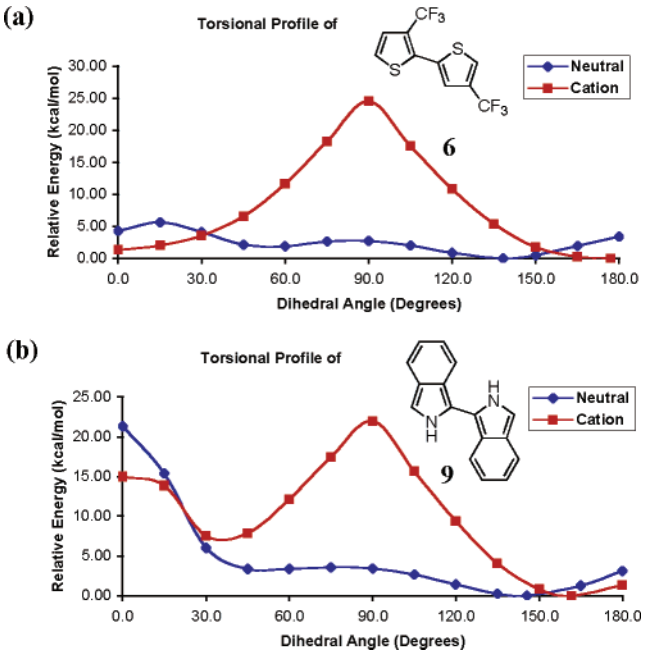

Figure 8. Torsional profiles of neutral and cationic oligomers: (a) molecular pair **6** and (b) molecular pair **9**, showing the inter-ring rotational barriers and differences in relative energies between the optimized geometries of neutral and cationic oligomers. The rotational energy contributions are 57% and 31% of the total internal reorganization energies for molecular pairs **6** and **9**, respectively.

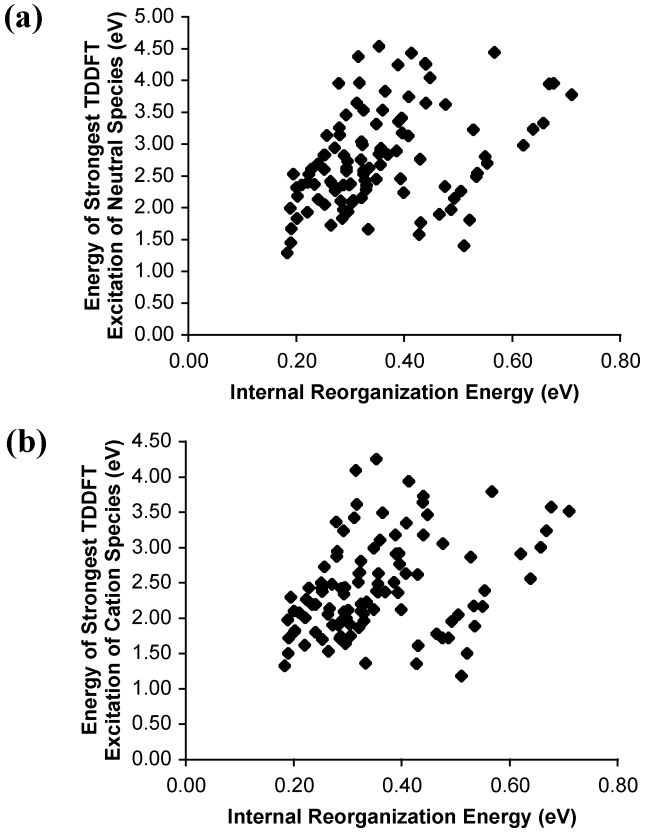

Figure 9. Comparisons between computed internal reorganization energies and the largest oscillator-strength computed TDDFT excitation energies for all oligomers in Figure 2 in the (a) neutral and (b) cation species. TDDFT excitation energies from ref 24. Note marginal correlation for either charge state.

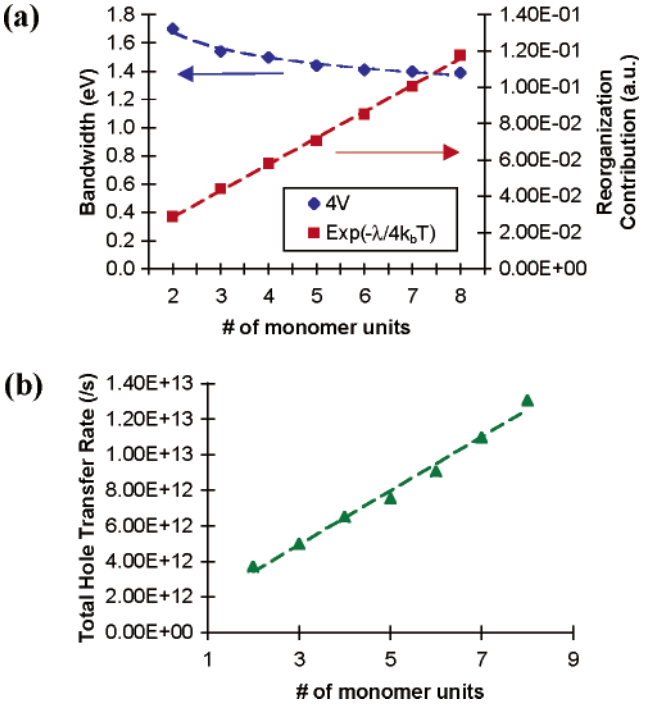

Figure 10. Comparison of oligothiophene **1** ($n = 2-8$): (a) bandwidth and reorganization energy contributions to the (b) total hole transfer rate, as calculated from eq 2 at 298 K. Bandwidths are computed from the orbital energy splittings in ref 11. Note that while interchain splittings for two cofacial π-stacked oligomers (and thus bandwidths and V^2) decrease with increasing oligomer length, the decrease in the reorganization energy barrier dominates, and the total hole transfer rate increases with increasing oligomer length.

These results imply that strategies for tailoring optical band gaps and reorganization energies are likely to be substantially different, but the minimal correlation between optical band gap and λ also implies that rational approaches to designing highly conductive small band gap (optically transparent) oligomers and polymers can be devised. In Figure 9, these substances clearly will lie toward the bottom left corner—those possessing strong optical excitations in the near-IR region (i.e., energies $\leq$ 1.7 eV) together with small internal reorganization energies to increase intrinsic hole transfer rates.

F. Comparisons of λ Effects on Total Charge-Transfer Rates. As noted above, the description in eqs 1 and 2 holds for both inter-oligomer/polymer and intra-oligomer/polymer charge transfer. We now focus on the inter-oligomer process. The computed internal reorganization energies range from 0.710 eV for the dimer of series **21** to 0.183 eV for the hexamer of series **16**. This range is consistent with gas-phase reorganization energies of fused-ring aromatic molecules measured via photoelectron spectroscopy[31] (in solution, the solvent reorganization energy often dominates the internal λ)[21]. Using eq 2, this range in computed reorganization energies yields a difference of over 2 orders of magnitude in the inverse exponential contribution to the total inter-oligomer hole transfer hopping rate at 298 K, assuming other factors remain constant (i.e., similar electronic coupling matrix elements). To produce a comparable difference in overall hole transfer rate, the electronic coupling matrix element must change by a factor of 13 at 298 K. This is greater than would be expected based on the similar $\pi-\pi$ intermolecular spacings found in typical oligothiophene crystal structures (Figure 10a).[11] Assuming relatively constant electronic coupling

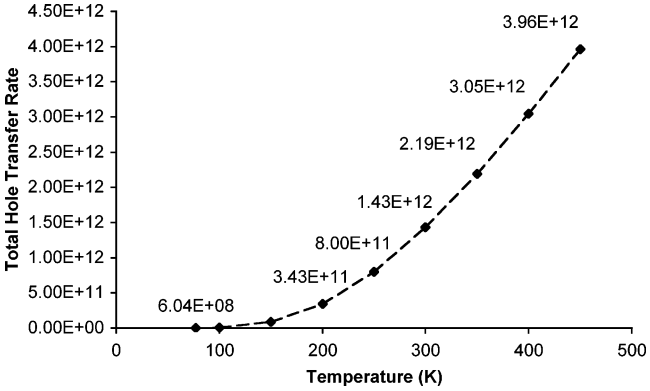

Figure 11. Predicted temperature dependence of the hole transfer rate for sexithiophene based on computed internal reorganization energies (with electronic coupling matrix elements (V) from orbital energy splittings in ref 11) for tilted π-stacks analogous to single-crystal oligothiophenes.

matrix elements across the series, the range in λ also indicates that all compounds studied would fall into the nonadiabatic charge-transfer model assumed in eq 2, as $V < \lambda$.

Figure 10 illustrates the response of the bandwidth (from the electronic coupling matrix element between two adjacent, cofacial π-stacked oligothiophene molecules)[11] and the $e^{-\lambda/4k_bT}$ factor (from the internal reorganization energies) to increasing oligomer length in oligothiophene series **1**. The electronic coupling matrix elements were computed from HOMO level splittings in the corresponding molecular dimers[11] and decrease with increasing oligomer length, as do the computed λ values. However, the *barriers represented by reorganization energies decrease* with increasing length as the charge delocalizes over more monomer units (Figure 10a) and thus, the overall hole transfer rates *increase* with increasing oligomer length (Figure 10b), since the exponential nature of the internal reorganization contribution dominates. While the $\pi-\pi$ derived level splittings are clearly important in addressing issues such as anisotropy of charge transfer and relative mobilities of holes vs electrons, trends in reorganization energies appear to dominate trends in intrinsic charge-transfer rates in organic conductive materials.

The drift mobility of hole-type hopping charges, μ, is given by the Einstein relation

$$\mu = \frac{e}{k_bT} D = \frac{eL^2 k_{hole}}{k_bT} \qquad (10)$$

where e is the electronic charge, D is the diffusion coefficient of charge carriers, and L is the separation between sites. Since the computed hole transfer rate is directly proportional to the hole mobility, the present calculated increase of this rate with increased oligomer length gratifyingly agrees with the experimentally observed increased mobilities of longer-length oligothiophenes in optimized OFET devices.[37] These computational results are also consistent with experimental trends in hole mobilities in solid-state arylamines.[19]

Since the reorganization barrier dominates the oligomer length dependence of overall hole transfer rates for short oligomers, there should also be a strong temperature dependence of the charge-transfer mobility, as illustrated in Figure 11. For sexithiophene, the computations predict an increase in temperature from 300 K to 350 K should increase the overall hole transfer rate by ~53%, while a decrease in temperature from 300 K to

200 K should decrease the overall hole transfer rate by ~76%, assuming that the charge transport mechanism remains constant and the intrinsic hole mobility discussed here is the dominant contributor to the experimental charge transfer mobility. At 77 K, the hole transfer rate is computed to be only 1/2400 of that at 300 K. As intrinsic hole transfer rates, these values should be most comparable to experimental measurements of the temperature-dependence of hole mobilities in single-crystal sexithiophene, since in a polycrystalline film, grain boundary effects may well be important.[38] Interestingly, in thin single-crystal sexithiophene measurements,[7] thermally activated hole transport is observed at temperatures above 100 K with an activation barrier of 0.025 eV, in reasonable agreement with the present computed gas-phase barrier ($\lambda/4$). This implies that the lattice environmental reorganization (akin to outer-sphere reorganization energy in solution-phase charge-transfer processes) is very small, as assumed above, otherwise the experimental activation barrier would be larger than the computed one.

Since large-displacement motions, such as torsions, are major contributors to λ_i, it is not surprising that the experimental λ values are somewhat smaller than the computed ones, because the structural constraints of the crystal environment may to some degree limit the possible displacements along these large-amplitude internal reorganization modes.[20] Furthermore, we have assumed in eq 2 that the thermal energy is sufficient to treat vibrational modes classically. Since conjugated CC stretching modes implicit in λ computed here are ~1500 cm^{-1}, this is not true and eq 2 is approximate—full quantum mechanical effects will lower the actual barrier. However, considering the reasonable agreement between computed and experimental activation barriers above, these effects appear to be minor and in fact would bring the computed values closer to that observed experimentally.

When comparing to other experimental activation barriers, the experimental sexithiophene barrier is significantly smaller than the 0.160 eV activation barrier measured for hole mobility in single-crystal tetraselenafulvalene,[9] corresponding to a λ_i ~0.64 eV—in the same range as many of the λ_i values computed here. In contrast, temperature-dependent measurements on single-crystal acenes[8] show a higher concentration of trap states and different temperature dependence for hopping transport.

IV. Conclusions

The necessary requirement for *electrically conductive* organic materials is the ability to transfer charge, either holes or electrons, between neighboring structural units. Therefore, we have considered a hopping-type transport mechanism in terms of hole transfer between two neighboring conjugated heterocyclic oligomers as an electron-transfer reaction, and have focused on the influence of molecular structure on computed internal reorganization energies.

In all-*trans*-oligoenes, the correlation between oligomer length and computed internal reorganization energy illustrates the effects of a self-localized polaron, since reorganization energies saturate at approximately 6−7 double bonds. In marked contrast, the computed λ for oligoheterocycles such as oligothiophenes, oligofurans, and oligopyrroles do not exhibit this saturation effect between 2 and 12 monomer units, but do exhibit a clear linear correlation between reorganization energy and the square root of the number of monomer units. Remarkably, this empirical correlation fits the various oligomer series in Figure 2 rather well, with the exception of those having isobenzo substitution (oligomers **2**, **9**, and **16**), which show little correlation between the computed internal reorganization energy and oligomer length. These isobenzo-substituted oligomers appear to strike a balance between decreasing reorganization energies arising from increased delocalization at longer oligomer lengths and the torsional contribution required to planarize an additional monomer unit in the transition between neutral and cation geometries.

While simple measures of geometric distortion, such as changes in bond length alternation and average inter-ring dihedral angles, contribute to computed internal reorganization energies, because these strictly geometric parameters do not completely take into account the energies required to induce structural deformations, they do not characterize the λ values as accurately as more elaborate models that combine the principal factors of oligomer length, heteroatom identity, and heterocycle substitutent. Such models better allow a priori estimation of reorganization energies for new materials, since they do not require measures of bond lengths and dihedral angles. The statistical analysis presented here illustrates that for many species, a significant contribution to the overall reorganization energy derives from differences between the inter-ring dihedral angles in the corresponding neutral and cation oligomer pairs. This contribution can account for up to 57% of the overall computed λ, and illustrates that steric crowding can lead to large reorganization energies, as is the case in trifluoromethyl- and amino-substituted oligomers.

Due to the range of computed reorganization energies within the diverse series of oligoheterocycle structures examined, we find that at 298 K, the computed intrinsic hole transfer rates can vary by over 2 orders of magnitude. Combined with prior estimates of the electronic coupling between π-stacked oligothiophenes, the present calculations show that the oligomer length-dependence of the intrinsic hole transfer rate in oligothiophenes of varying lengths is dominated by changes in the reorganization energy. This indicates that optimization of reorganization energy, and in particular, of the inter-ring torsional component, should lead to higher mobility organic conductors and semiconductors. This predicted dominance of the thermally activated reorganization barrier here also suggests that strongly temperature-dependent mobility should be observed if the charge transfer mechanism is invariant over a range of temperatures. This is in excellent agreement with activated-

(37) (a) Facchetti, A.; Mushrush, M.; Katz, H. E.; Marks, T. J. *Adv. Mater.* **2003**, *15*, 33. (b) Halik, M.; Klauk, H.; Zschieschang, U.; Schmid, G.; Ponomarenko, S.; Kirchmeyer, S.; Weber, W. *Adv. Mater.* **2003**, *15*, 917. (c) Horowitz, G.; Hajlaoui, R.; Fichou, D.; El Kassmi, A. *J. Appl. Phys.* **1999**, *85*, 3202. (d) Katz, H. E.; Torsi, L.; Dodabalapur, A. *Chem. Mater.* **1995**, *7*, 2235. (e) Horowitz, G.; Peng, X. Z.; Fichou, D.; Garnier, F. *J. Mol. Electron.* **1991**, *7*, 85. (f) Facchetti, A.; Mushrush, M.; Yoon, M.-H.; Hutchison, G. R.; Ratner, M. A.; Marks, T. J. *J. Am. Chem. Soc.* **2004**, *126*, 13859.

(38) (a) Chwang, A. B.; Frisbie, C. D. *J. Appl. Phys.* **2001**, *90*, 1342. (b) Kelley, T. W.; Frisbie, C. D. **2001**, *105*, 4538. (c) Schon, J. H.; Batlogg, B. **2001**, *89*, 336. (d) Horowitz, G.; Hajlaoui, M. E. **2000**, *12*, 1046. (e) Schon, J. H.; Batlogg, B. **1999**, *74*, 260. (f) Nussbaumer, H.; Baumgartner, F. P.; Willeke, G.; Bucher, E. **1998**, *83*, 292. (g) Ling, C. H. **1984**, *27*, 633. (h) Levinson, J.; Shepherd, F. R.; Scanlon, P. J.; Westwood, W. D.; Este, G.; Rider, M. **1982**, *53*, 1193. (i) Seager, C. H.; Pike, G. E. **1979**, *35*, 709. (j) Pike, G. E.; Seager, C. H. **1979**, *50*, 3414. (k) Seager, C. H.; Castner, T. G. **1978**, *49*, 3879. (l) Torsi, L.; Dodabalapur, A.; Rothberg, L. J.; Fung, A. W. P.; Katz, H. E. *Phys. Rev. B* **1998**, *57*, 2271. (m) Horowitz, G.; Hajlaoui, M. E.; Hajlaoui, R. *J. Appl. Phys.* **2000**, *87*, 4456. (n) Horowitz, G.; Hajlaoui, M. E. *Synth. Met.* **2001**, *121*, 1349.

transport observed in single-crystal sexithiophene, albeit with a slightly lower activation barrier, perhaps due to lower reorganization energies in the solid state and the classical charge-transfer model used here. The small difference between the two also implies that environmental reorganization of the lattice itself must be small.

Acknowledgment. We thank the NSF/MRSEC program through the Northwestern MRSEC (NSF DMR-0076097), the ONR (N00014-02-1-0909), and the NASA Institute for Nanoelectronics and Computing (Award NCC 2-3163) for support.

JA0461421